Published in final edited form as:
Biochemistry. 2012 June 19; 51(24): 4888–4897. doi:10.1021/bi300517s.

Mechanistic and Structural Analyses of the Role of His67 in the Yeast Polyamine Oxidase Fms1[†]

Mariya S. Adachi[‡], **Alexander B. Taylor**[‡], **P. John Hart**[‡,§], and **Paul F. Fitzpatrick**[‡,*]

[‡]Department of Biochemistry, University of Texas Health Science Center, San Antonio, TX 78229

[§]Department of Veterans Affairs, Audie Murphy Division, Geriatric Research, Education, and Clinical Center, South Texas Veterans Health Care System, San Antonio, TX 78229

Abstract

The flavoprotein oxidase Fms1 from *Saccharomyces cerevisiae* catalyzes the oxidation of spermine and N^1-acetylspermine to spermidine and 3-aminopropanal or N-acetyl-3-aminopropanal. Within the active site of Fms1, His67 is positioned to form hydrogen bonds with the polyamine substrate. This residue is also conserved in other polyamine oxidases. The catalytic properties of H67Q, H67N, and H67A Fms1 have been characterized to evaluate the role of this residue in catalysis. With both spermine and N^1-acetylspermine as the amine substrate, the value of the first-order rate constant for flavin reduction decreases 2–3 orders of magnitude, with the H67Q mutation having the smallest effect and H67N the largest. The k_{cat}/K_{O2} value changes very little upon mutation with N^1-acetylspermine as the amine substrate and decreases only an order of magnitude with spermine. The k_{cat}/K_M-pH profiles with N^1-acetylspermine are bell-shaped for all the mutants; the similarity to the profile of the wild-type enzyme rules out His67 as being responsible for either of the pK_a values. The pH profiles for the rate constant for flavin reduction for all the mutant enzymes similarly show the same pK_a as wild-type Fms1, about ~7.4; this pK_a is assigned to the substrate N4. The k_{cat}/K_{O2}-pH profiles for wild-type Fms1 and the H67A enzyme both show a pK_a of about ~6.9; this suggests His67 is not responsible for this pH behaviour. With the H67Q, H67N, and H67A enzymes the k_{cat} value decreases when a single residue is protonated, as is the case with the wild-type enzyme. The structure of H67Q Fms1 has been determined at a resolution of 2.4 Å. The structure shows that the mutation disrupts a hydrogen bond network in the active site, suggesting that His67 is important both for direct interactions with the substrate and to maintain the overall active site structure.

INTRODUCTION

Flavoprotein amine oxidases catalyze the oxidation of amino acids and amines (3). Most flavoprotein amine oxidases can be placed into one of two structural groups. The D-amino acid oxidase (DAAO)[1] family contains DAAO (4) and enzymes that oxidize glycine or *N*-methylated amino acids (5–8). The monoamine oxidase (MAO) family contains MAO A and B (9, 10), histone lysine demethylase (11), the L-amino acid oxidases (12), and the spermine and polyamine oxidases (1), including yeast Fms1 (13).

[†]This work was supported in part by the NIH, grant GM058698 (to PFF), and The Welch Foundation, grants AQ-1399 (to PJH) and AQ1245 (to PFF).

[*]To whom correspondence should be addressed: Department of Biochemistry, University of Texas Health Science Center, San Antonio, TX 78229. Phone: (210) 567-8264. Fax: (210) 567-8778. fitzpatrick@biochem.uthscsa.edu.

[1]Abbreviations used: DAAO, D-amino acid oxidase; MAO, monoamine oxidase; SMO, spermine oxidase; PAO, polyamine oxidase; Ni-NTA, nickel-nitrilotriacetic acid.

Fms1, along with polyamine and spermine oxidases, is involved in the catabolism of polyamines in cells (Scheme 1) (14, 15). In general, spermine oxidases (SMOs) preferentially oxidize spermine (16), while polyamine oxidases (PAOs) prefer N^1-acetylspermine and N^1-acetylspermidine (17). Fms1 is intermediate in its specificity in that it is capable of oxidizing both spermine and N^1-acetylspermine, with only a small preference for the latter (18). The structural basis for the differences in specificity among these enzymes is not known, as no structures are available of SMOs or PAOs from animal sources. In contrast, there is a crystal structure of yeast Fms1 that shows the protein has a fold similar to that of MAO (13). As shown in Figure 1, much of the binding site for the polyamine in Fms1 is made up of hydrophobic or aromatic residues, with only three polar residues in the vicinity of the substrate[2]. His67 is positioned to interact with N4 of spermine, while Asn195 and Asp94 could interact with the substrate N14. Alignment of the sequences of the yeast Fms1 and human and mouse SMO and PAO shows that all these enzymes have a conserved histidine residue that corresponds to His67 in Fms1.

The overall catalytic reactions of flavoprotein oxidases such as Fms1 can be divided into reductive and oxidative half-reactions (Scheme 2). In the reductive half-reaction, binding of the oxidized substrate is followed by transfer of a hydride equivalent to the flavin to form reduced flavin and oxidized substrate. In the oxidative half-reaction, the reduced flavin is oxidized by molecular oxygen to form H_2O_2; the oxidized amine then dissociates from the enzyme. The pH profiles for the reductive half-reactions of Fms1, human SMO, and mouse PAO all show that a moiety with a pK_a value of 7.2–8.3 must be unprotonated for amine oxidation (19–21). This pK_a value has been attributed to either N4 of the polyamine substrate in the enzyme-substrate complex or a residue in the active site of the protein. Based on the structure of Fms1, His67 is a likely candidate for this critical active site residue. We describe here the effects of replacing His67 of Fms1 with glutamine, asparagine, and alanine on specificity and catalysis.

MATERIALS AND METHODS

Materials

Spermine was purchased from Acros Organics (Geel, Belgium). N^1-Acetylspermine trihydrochloride, glycerol, and glucose oxidase were from Sigma-Aldrich (Milwaukee, WI). HEPES and sucrose were from Fisher (Pittsburg, PA). The nickel-nitrilotriacetic acid (Ni-NTA) agarose and the Sephacryl S-100 HR resin were purchased from Invitrogen (Carlsbad, CA) and Sigma-Aldrich (Milwaukee, WI), respectively.

DNA Manipulations

The pJWL94 plasmid previously used for expression of wild-type Fms1 (18) was used as the template for construction of plasmids for expression of the mutant enzymes. The H67N, H67Q, and H67A mutations were generated with the QuikChange protocol (Stratagene). The protein-coding region of the plasmids used for protein expression was sequenced to ensure that no unwanted mutations were incorporated during the polymerase chain reaction. DNA sequencing was performed at the Nucleic Acid Core Facility at the University of Texas Health Science Center at San Antonio.

[2]Due to weak electron density, the position of N1 of spermine is not well-defined in the structure of the Fms1-spermine complex, pdb file 1xpq. This is consistent with the high thermal parameters reported for spermine, which are 3–5 times greater than those of the protein atoms in the refined structure. It may reflect the effects of the pH at which the crystals were grown, pH 5.6. While plant PAOs oxidize a different carbon-nitrogn bond from the animal enzymes, there are structures of the polyamine oxidase from maize (1), including a structure of a mutant enzyme in complex with spermine (2). The binding site for spermine identified in the latter structure generally agrees with that proposed for Fms1, although the residues interacting with the substrate in the two proteins are not conserved.

Protein Expression and Purification

The wild-type Fms1 and mutant enzymes used for steady-state and rapid-reaction kinetics were expressed and purified following the wild-type enzyme protocol (21). For crystallization of the H67Q enzyme, after the Ni-NTA column the enzyme was dialyzed against three changes of 25 mM potassium phosphate (pH 7.5), 25 mM NaCl, 10% glycerol and loaded onto a Sephacryl S-100 HR gel filtration column. The protein was eluted with the same buffer. Fractions containing pure enzyme were pooled and concentrated to 17–20 mg/ml using 30K Amicon Ultra Centrifugal filters. The purified protein was dialyzed against four changes of 25 mM HEPES (pH 7.5).

Assays

Enzyme activities were determined in buffer containing 10% glycerol by following oxygen consumption with a Yellow Springs Instrument Model 5300 oxygen monitor at 25 °C. All assays were initiated by the addition of enzyme. Buffers were 200 mM Tris-HCl from pH 7.0 to 8.75, 200 mM CHES from pH 9.0 to 9.75, and 200 mM CAPS from pH 10.1 to 10.5. For assays not performed in air-saturated buffer, the appropriate O_2/N_2 mixture was bubbled into the cell of the oxygen electrode for 10 min prior to starting the reaction by adding enzyme. The k_{cat} values were determined by varying either spermine or N^1-acetylspermine while the oxygen concentration was at 1.3 mM. To determine k_{cat}/K_{O2} values, the concentration of oxygen was varied from 64 μM to 1.3 mM at an amine concentration 10 times the K_M value. Due to the hygroscopic nature of N^1-acetylspermine, its concentration was determined enzymatically. The absolute viscosities (η) for buffers containing either glycerol or sucrose were obtained from the literature (22).

Rapid-Reaction Kinetics

Rapid-reaction kinetic measurements were performed at 25°C with an Applied Photophysics SX-20MV stopped-flow spectrophotometer in the absorbance mode. The instrument, enzyme and substrate solutions were made anaerobic as described previously (21). For pH-profiles the buffers were 200 mM PIPES at pH 6.5, 200 mM Tris-HCl from pH 7.0 to 8.5, and 200 mM CHES from 9.0 to 9.7.

Data Analysis

Kinetic data were analyzed using the program KaleidaGraph (Adelbeck Software, Reading, PA). The steady-state kinetic parameters k_{cat}, k_{cat}/K_M, and K_M were determined by fitting the data to the Michaelis-Menten equation. Eq 1 was used to analyze the pH-dependence of kinetic parameters that decreased at both low and high pH. Data for the k_2-pH profiles were fit to eq 2, which applies for a kinetic parameter that decreases only at low pH. In these equations, K_1 and K_2 are the dissociation constants for the ionizable groups, and C is the pH-independent value of the kinetic parameter of interest. Eq 3 was used to fit the k_{cat}-pH profile for all mutant enzymes. This equation describes a kinetic parameter that decreases to a limiting value at low pH. In this equation, Y_L and Y_H are the values of the kinetic parameter at the pH extremes, and K_1 is the pK_a of the group whose ionization or protonation decreases activity (23). For rapid-reaction studies of enzyme reduction, transient changes in absorbance were fit to eq 4, which describes a biphasic exponential decay. Here, λ_1 and λ_2 are the first-order rate constants for each phase, A_1 and A_2 are the absorbances of each species at time t, and A_8 is the final absorbance. The concentration dependence of the measured rate constant for reduction by the amine substrate was fit to eq 5, where k_{obs} is the observed rate constant, k_2 is the rate constant for reduction at saturating concentrations of the amine, and K_d is the apparent dissociation constant for the enzyme-amine complex. The Arrhenius equation (eq 6) was used to extrapolate to 25 °C values of k_2 determined as a

function of temperature from 4-15 °C. Here, A is the prefactor, R is the gas constant, E_a is activation energy, and T is the temperature.

$$\log Y = \log\left(\frac{C}{1+\frac{H}{K_1}+\frac{K_2}{H}}\right) \quad (1)$$

$$\log Y = \log\left(\frac{C}{1+\frac{H}{K_1}}\right) \quad (2)$$

$$\log Y = \log\left(\frac{Y_L + Y_H\frac{K_1}{H}}{1+\frac{K_1}{H}}\right) \quad (3)$$

$$A = A_\infty + A_1 e^{-\lambda_1 t} + A_2 e^{-\lambda_2 t} \quad (4)$$

$$k_{obs} = \frac{k_2 S}{K_d + S} \quad (5)$$

$$k_2 = A e^{-Ea/RT} \quad (6)$$

Crystallization, Structure Determination, and Refinement

Crystals of the FMS1 H67Q variant were grown in the UTHSCSA X-ray Crystallography Core Laboratory from commercial crystallization screen kits (Qiagen Inc., Valencia, CA) using a Phoenix crystallization robot (Art Robbins Instruments, Sunnyvale, CA). The crystals grew within one week using the sitting drop vapor diffusion method with the protein solution (~20 mg/ml in 25 mM HEPES (pH 7.5)) mixed in a 1:1 ratio with a buffer containing 20% (w/v) polyethylene glycol 3350, 0.2 M sodium acetate and 0.1 M bis-Tris propane (pH 7.5). Diffraction data were collected from crystals flash-cooled with liquid nitrogen at beamline 24-ID-C at the Advanced Photon Source, Argonne, IL. The data were integrated using XDS (24) and scaled using SCALA (25). Phases were generated by the molecular replacement method as implemented in PHASER (26) using FMS1 coordinates in Protein Data Bank entry 1RSG (13) as the search model. Coordinates were refined against the diffraction data using PHENIX (27) including simulated annealing, and alternated with manual rebuilding using COOT (28). Data collection and refinement statistics are listed in Table 1. The coordinates have been deposited in the Protein Data Bank with accession code 4ECH.

RESULTS

Steady-State Kinetic Parameters

To analyze the role of His67 of Fms1 in binding and catalysis, this residue was mutated to glutamine, asparagine, and alanine. The steady-state kinetic parameters of the mutant enzymes with both spermine and N^1-acetylspermine as the substrates are given in Table 2. The analyses were carried out at the respective pH optima, 9.35 for spermine and 9.0 for N^1-acetylspermine (see below). The k_{cat}/K_M value for N^1-acetylspermine oxidation only decreased about 20-fold with all three mutant enzymes in comparison to the wild-type value.

In contrast, the k_{cat}/K_M value for spermine oxidation decreased about 100- and 1300-fold with the H67Q and H67A enzymes, respectively. With the H67N enzyme spermine oxidation was too slow to measure a k_{cat}/K_M value. The much larger effect of the mutation on the k_{cat}/K_M value for spermine resulted in an increase in the specificity for N^1-acetylspermine over spermine as a substrate for the mutant enzymes, from 4-fold for wild-type Fms1, to 23- and 220-fold for the H67Q and H67A enzymes.

The effects of the mutations on the oxidative half-reaction were smaller. In the reaction with N^1-acetylspermine the k_{cat}/K_{O2} value decreased only 6-fold for the H67N and H67A enzymes and did not decrease significantly (about 1.6-fold) for the H67Q enzyme. In the reaction with spermine the k_{cat}/K_{O2} values decreased 16- and 35-fold for the H67Q and H67A enzymes, respectively. The k_{cat} value similarly showed a much larger effect with spermine as substrate, decreasing 2–3 orders of magnitude compared to decreases of 5 to 10-fold with N^1-acetylspermine.

Effect of pH on the Steady-State Kinetic Parameters

The effects of mutating His67 on the k_{cat}/K_M, k_{cat}/K_{O2}, and k_{cat}-pH profiles were determined with N^1-acetylspermine as the amine substrate. For all three mutant enzymes the k_{cat}/K_M-pH profiles are bell-shaped, with maxima of ~9.0, similar to the profile for the wild-type enzyme (Figure 2). These pH profiles show the importance of two ionizable groups in the free enzyme or substrate, one of which must be protonated and one unprotonated for full activity. The data were fit to eq 1 to extract the pK_a values (Table 3). The separation of the acidic and basic limbs of the profile decreases with decreasing activity of the mutant enzyme. Only for the H67Q enzyme are the two pK_a values separated sufficiently to obtain discrete pK_a values; for the H67N and H67A enzymes the two pK_a values are too close together to resolve, so that only the average pK_a value of the two ionizable groups could be determined.

The k_{cat}/K_{O2}-pH profile was only determined for the H67A mutant, since it is the least conservative mutation. As shown in Figure 3, the effect of pH on the k_{cat}/K_{O2} value with N^1-acetylspermine as the amine substrate decreases from a constant value at high pH, indicating the importance of a single group that must be unprotonated for full activity. The shape of the profile for this mutant matches that of the wild-type enzyme, with the data for both enzymes yielding the same pK_a value when fit to eq 2 (Table 3).

The effects of pH on k_{cat} values were determined with all three mutant enzymes, again using N^1-acetylspermine as the amine substrate. The results are shown in Figure 4. With all four enzymes the k_{cat} value is constant at high pH but decreases to a constant lower value at low pH. To obtain the pK_a values for the decrease in activity (Table 3), the data were fit to eq 3. This gave comparable pK_a values near 8 for all four enzymes, with the pK_a value decreasing slightly as the k_{cat} value decreased (Table 3).

Effect of Solvent Viscosity

The narrowing of the k_{cat}/K_M-pH profile (Figure 2) seen with the mutant enzymes suggested that there is a significant forward commitment to catalysis with the wild-type enzyme (29). The possibility that binding of N^1-acetylspermine partially limits the reductive half-reaction was investigated by measuring the effect of solvent viscosity on the k_{cat}/K_M value (30). In initial experiments both glycerol and sucrose were used as viscogens. However, the k_{cat} values for both wild-type Fms1 and the H67A enzyme increased slightly in the presence of high concentrations of glycerol. Therefore, only sucrose was used as a viscogen. The effects of sucrose on the steady-state kinetic parameters for both wild-type Fms1 and the H67A enzyme are shown in Figure 5, in which the relative k_{cat}/K_M value is plotted as a function of

the relative viscosity. The sensitivity of this kinetic parameter to viscosity can be calculated from a slope of such a plot. A slope of zero means a parameter is independent of solvent viscosity, whereas a slope of 1 means a completely diffusion-limited reaction. Figure 5 shows that the k_{cat}/K_M value decreases with increasing viscosity, with the H67A enzyme being less sensitive to viscosity than the wild type enzyme, 11 ± 2% versus 35 ± 8%.

Rapid-Reaction Kinetics

The rate constant for flavin reduction was determined for the H67Q, H67N, and H67A enzymes in single-turnover experiments by following the changes in the flavin absorbance at 458 nm when the enzyme is mixed with an amine substrate in the absence of oxygen. The decrease in absorbance upon mixing the H67Q and H67A enzymes with either substrate was biphasic, with most of the absorbance change occurring in the more rapid first phase, as is the case with the wild-type enzyme (21). Similar results were obtained upon mixing the H67N enzyme with N^1-acetylspermine, but mixing this enzyme with spermine in the absence of oxygen produced no spectral changes. For all the mutant enzymes only the first order rate constant for the fast phase was substrate-dependent, similar to the behavior of wild-type Fms1 and consistent with the kinetic mechanism of Scheme 3. Here, binding of the substrate to the enzyme is followed by reduction of the flavin and oxidation of the amine substrate in a single first-order step. The apparent K_d value for binding of the amine substrate to the oxidized enzyme and the rate constant for reduction, k_2, can be determined from the concentration dependence of this pseudo-first order rate constant using eq 5. The product slowly dissociates from the reduced enzyme with a rate constant slower than turnover. This slow step is not along the normal catalytic pathway, which involves product release from the oxidized enzyme. The k_2, k_3, and apparent K_d values for the mutant enzymes determined from these analyses are listed in Table 4.

The k_2 value for N^1-acetylspermine oxidation by the wild-type Fms1 was previously determined at 4 °C (21) because it is too fast to measure at 25 °C. To allow comparison to the k_2 values for the His67 mutants determined at 25 °C, the k_2 value for the wild-type enzyme was determined as a function of temperature from 4–15 °C and then extrapolated to 25 °C using the Arrhenius equation, yielding a k_2 value of 5500 s^{-1}. This analysis also yielded an E_a value for amine oxidation by Fms1 of 9.5 ± 3.0 kcal/mol. With N^1-acetylspermine as the amine substrate, the value of k_2 decreases about 100-, 400-, and 2100-fold with the H67Q, H67A, and H67N enzymes, respectively, compared to the value for the wild-type enzyme. The apparent K_d values for the mutant enzymes are essentially equal and about 20–30-fold lower than that for wild-type Fms1. With spermine as substrate, the value of k_2 similarly decreases significantly for the H67Q and H67A enzymes, 60- and 210-fold, respectively, while the K_d value increases 10- and 140-fold for the H67A and H67Q enzyme, respectively.

With N^1-acetylspermine as a substrate, the rate constant for the slow phase (k_3 in Scheme 3) has identical values for wild-type Fms1 and the H67Q and H67A enzymes. With spermine as a substrate, the value of k_3 decreases 45- and 900-fold with the H67Q and H67A enzymes, respectively.

The effect of pH on the rate constants for the reductive half-reaction was determined for the H67Q and H67N enzymes with N^1-acetylspermine as a substrate. The k_2-pH profiles are shown in Figure 6. With both wild-type Fms1 and the mutant enzymes, the value of k_2 is pH-independent at high pH and decreases at low pH. The data were fit to eq 3 to obtain the pK_a value (Table 3) for the moiety that must be unprotonated for reduction. With both mutant enzymes the pK_a value is unchanged from the wild-type value.

Crystal Structure of H67Q Fms1

To determine how mutation of His67 affected the structure of Fms1, we determined the three-dimensional structure of Fms1 H67Q by X-ray crystallography. The data collection and refinement statistics are reported in Table 1. The crystallization conditions, different from those used for the wild-type enzyme (13), yielded crystals that diffracted to 2.4 Å resolution. The overall structure of the mutant protein was superimposable on that of the wild-type enzyme, with an RMSD of 0.39 Å for the a carbons in 482 residues. As shown in Figure 7, the active site, including the FAD and the glutamine at position 67, were well-defined by the electron density. Efforts to obtain a structure with spermine bound were unsuccessful, in that addition of spermine resulted in non-diffracting crystals. As with the wild-type enzyme, residues 343–348 were disordered in the crystals of H67Q Fms1; this surface loop is also absent in the structure of Fms1 with spermine (13). In addition, the structure of the mutant lacked surface loops containing residues 419–426 and 132–133; these two loops have different positions in the structures of Fms1 with and without spermine.

Figure 8 compares the positions of active site residues in the mutant and wild-type enzymes. The glutamine residue in the mutant protein is superimposable on His67 in the wild-type enzyme (Figure 8A). In the wild-type enzyme there is a hydrogen bond interaction between the δ nitrogen of His67 and the side chain of Asn195; this would be disrupted in the mutant enzyme, since the distance between these residues increases to 4.7 Å. The positions of Trp174, Phe189, and His191 in the mutant enzyme differ from those in the wild-type enzyme (Figure 8B). The indole ring of Trp174 has been proposed to form one side of the binding site for the central butyl moiety of spermine (13). In the mutant enzyme, the indole ring of Trp174 protrudes into the binding site for spermine. The significance of this difference is unclear. Different rotamers of Trp174, Phe189, and His191 are also found in the structures of the wild-type enzyme with and without spermine. This suggests that all three residues are mobile in the absence of substrate, and therefore the differences in the position of Trp174 between the mutant and wild-type protein do not reflect functionally meaningful changes due to the mutation.

DISCUSSION

Mutagenesis of His67 in Fms1 has significant effects on the kinetic parameters of the enzyme, establishing this residue as critical for catalysis. The combination of steady-state and rapid-reaction kinetic data for the His67 mutant enzymes described here allows determination of the effects of the mutations on each of the kinetic constants in the mechanism of Scheme 2 (Table 4) (21). The apparent K_d values and the first-order rate constants for amine oxidation (k_2) can be directly measured in the stopped-flow spectrophotometer. The value for k_4 corresponds to the k_{cat}/K_{O2} value, and the value of k_5 can be calculated.

The greatest effect of mutating His67 on enzyme activity is on the rate constant for amine oxidation (k_2). Mutagenesis of this residue to glutamine decreases this rate constant by almost 100-fold with either N^1-acetylspermine or spermine as substrate, while the less conservative alanine and asparagine mutations decrease the value even more. The k_{cat}/K_M values for both polyamine substrates decrease in the mutant enzymes. The effects of the mutations on the k_{cat}/K_M value for spermine agree reasonably well with the effects on the k_2 values, consistent with the k_{cat}/K_M value reflecting the rate constants for all of the steps from free enzyme and substrate through oxidation of the amine. The increases in the apparent K_d value for spermine for the mutant enzymes are consistent with binding of this substrate being somewhat disrupted upon mutation of His67. In contrast, the effects on the k_{cat}/K_M value for N^1-acetylspermine are much less than the effects on the k_2 value, while

the apparent K_d values decrease. These results suggest that the k_{cat}/K_M value for the wild-type enzyme with this substrate is limited not by chemistry but by association of N^1-acetylspermine with the enzyme. In other words, there is a significant forward commitment with this substrate for the wild-type enzyme. As a result, the apparent K_d value for this substrate determined from single turnover data is larger than the actual dissociation constant, while the changes in the k_2 are masked. The presence of a significant commitment for the wild-type enzyme with N^1-acetylspermine is supported by the effect of viscosity on the k_{cat}/K_m value and by the broader k_{cat}/K_m-pH profile (29).

The oxidative half-reaction is affected much less by mutation of His67 than the reductive half reaction. The reaction of the reduced Fms1-product complex with oxygen occurs in a single pseudo-first-order process with no detectable intermediates (21). Kinetically, with both substrates the reaction behaves as a simple second-order reaction with a rate constant (k_4) equal to the k_{cat}/K_{O2} value (Scheme 2). The k_{cat}/K_{O2} changes very little when N^1-acetylspermine is the amine substrate and decreases about an order of magnitude with spermine. The rate constants for the reactions of reduced flavoproteins have been found to be sensitive to the presence of positive charges near the flavin. The role of the charge is likely stabilization of the negative charge on oxygen as it is reduced. In the case of glucose oxidase, mutagenesis of an active site histidine decreases the rate constant for flavin oxidation by 2600-fold (31). For the structurally related enzyme choline oxidase, mutagenesis of the conserved histidine does not alter the k_{cat}/K_{O2} value (32) but elimination of the positively charged on the nitrogen of the substrate decreases it 75-fold (33). In the case of sarcosine oxidase, a member of a different structural family of flavoprotein oxidases, mutagenesis of an active site lysine residue decreases the rate constant for enzyme oxidation by ~10,000-fold (34, 35). The changes seen in the Fms1 His67 mutants are much smaller, ruling out one role of His67 being to provide a positive charge during flavin oxidation. Instead, the changes may reflect slightly altered binding of the bound product such that the positively-charged polyamine nitrogens contribute less to an overall positively charged environment around the flavin N5.

The rate constant for product release (k_5) was not measured directly. However, it is possible to calculate the value of this rate constant. For the mechanism of Scheme 2, $1/k_{cat} = 1/k_2 + 1/k_5$. The resulting values (Table 4) suggest that with N^1-acetylspermine as substrate, the k_{cat} values for the H67A and H67Q enzymes predominantly reflect the rate constants for product release, as is the case for the wild-type enzyme, and that the value of k_5 has decreased about 4-fold. For the H67N enzyme with N^1-acetylspermine and with both the H67Q and H67A enzymes with spermine as substrate, the values of k_2 and k_{cat} are comparable, suggesting that reduction is rate-limiting with these mutant enzymes.

The bell-shaped k_{cat}/K_{amine}-pH profiles for wild-type Fms1 were previously interpreted as arising from a strong preference for the doubly charged forms of polyamine substrates (21). Still, those data could not rule out the possibility that one or both of the pK_a values are due to an active site residue. The finding that the k_{cat}/K_{amine}-pH profiles for the mutant enzymes are also bell-shaped with essentially the same pH optimum as the wild-type enzyme rules out His67 as being responsible for either pK_a, consistent with the previous assignment of both to the free substrate. The narrowing of the k_{cat}/K_M-pH profiles seen with the mutant enzymes can be explained by a significant forward commitment to catalysis with wild-type Fms1 with N^1-acetylspermine as substrate.

The k_2-pH profiles for both the H67Q and the H67N enzymes with N^1-acetylspermine as substrate exhibit the same pK_a of about ~7.4 for a group that must be unprotonated for reduction seen in wild-type Fms1 (21). The fact that this pK_a value does not change rules out the possibility that it is due to His67. Thus, the pK_a seen in N^1-acetylspermine oxidation

catalyzed by Fms1 is most likely due to N4 of the substrate, which must be neutral for the amine to be oxidized. It is likely that the pK_a of His67 is outside the accessible pH range when an amine substrate is bound. This would set the pK_a of this residue at less than 6 or more than 10. The former is more likely, suggesting that His67 must be uncharged for the most favorable interaction with the substrate and Asn195.

The k_{cat}/K_{O2}-pH profiles for the wild-type Fms1 and H67A enzyme are similar and consistent with a need for a moiety in the reduced enzyme-product complex to be uncharged for rapid oxidation of the flavin (Figure 3). These results suggest that His67 is not responsible for this pH behavior. Mouse PAO shows a similar pK_a of 7.0 in the k_{cat}/K_{O2}-pH profile with N^1-acetylspermine as substrate (36), close to the value of 6.8 for wild-type Fms1. This pK_a is not seen when Lys315 in PAO is mutated to methionine. Lys315 in mouse PAO corresponds to a lysine residue that is conserved throughout the MAO/PAO family. Structures of several family members show that the amino group of this lysine forms a water-mediated hydrogen bond with the N5 of the FAD (1, 36). Lys296 of Fms1 corresponds to PAO Lys315, suggesting that the pK_a in the k_{cat}/K_{O2}-pH profile for Fms1 is due to Lys296.

The pH-k_{cat} profiles establish that the protonation of a group in the oxidized enzyme-product complex decreases the rate constant for release of the product from the oxidized enzymes, so that the conformational change required for product release is pH-dependent. A similar pH-dependent release of the oxidized amine product has been described for several flavoprotein amine oxidases, including DAAO (37, 38), and mouse PAO (36). Mutating either Lys315 in PAO or His67 in Fms1 has little effect on the k_{cat}-pH profile, ruling out the conserved lysine and histidine as the sources of the pK_a.

The structure of the H67Q enzyme establishes that the mutation does not have a significant effect on the overall structure of the protein. In the structure of the wild-type enzyme, His 67 is appropriately positioned to interact with substrate N1 and N4. The mechanism of this amine oxidation for the MAO family has been intensively studied (3, 39, 40) and a mechanism of direct hydride transfer from the amine substrate to the flavin is most consistent with the data (19–21, 41–44). Thus, His67 is unlikely to play a role as an active-site acid or base during amine oxidation. Instead, the likely role of this residue is to properly position the substrate for hydride transfer to the flavin. Figure 1 shows that His67 forms a hydrogen bond with Asn195; the latter residue can form a hydrogen bond with N14 of the substrate. In the H67Q enzyme, the glutamine residue is no longer able to form a hydrogen bond with Asn195. The loss of this hydrogen bond would be expected to further disrupt substrate binding, since the side chain of Asn195 would no longer be held in the proper position for interacting with the substrate.

In conclusion, the present results establish that His67 plays a critical role in properly positioning the polyamine substrate in the active site of Fms1. It is likely that the analogous residues in other animal polyamine oxidases play a similar role. In addition, the effects of pH on the kinetics of the mutant enzymes support the previous interpretation of the effects of pH on the kinetics of the wild-type enzyme, that the pK_a values seen in the k_{cat}/K_m and k_2 pH profiles reflect the ionization of the free and bound substrate rather than amino acid residues in the enzyme.

Acknowledgments

This material is based upon work supported in part by the Department of Veterans Affairs, Veterans Health Administration, Office of Research Development, Biomedical Laboratory Research and Development. Support for the X-ray Crystallography Core Laboratory by the UTHSCSA Executive Research Committee and the Cancer Therapy Research Center is gratefully acknowledged. This work is based upon research conducted at the Advanced

Photon Source on the Northeastern Collaborative Access Team beamlines, which are supported by grants from the National Center for Research Resources (5P41RR015301-10) and the National Institute of General Medical Sciences (8 P41 GM103403-10) from the National Institutes of Health. Use of the Advanced Photon Source, an Office of Science User Facility operated for the U.S. Department of Energy (DOE) Office of Science by Argonne National Laboratory, was supported by the U.S. DOE under Contract No. DE-AC02-06CH11357.

References

1. Binda C, Coda A, Angelini R, Federico R, Ascenzi P, Mattevi A. A 30 Å long U-shaped catalytic tunnel in the crystal structure of polyamine oxidase. Structure. 1999; 7:265–276. [PubMed: 10368296]
2. Fiorillo A, Federico R, Polticelli F, Boffi A, Mazzei F, Di Fusco M, Ilari A, Tavladoraki P. The structure of maize polyamine oxidase K300M mutant in complex with the natural substrates provides a snapshot of the catalytic mechanism of polyamine oxidation. FEBS Journal. 2011; 278:809–821. [PubMed: 21205212]
3. Fitzpatrick PF. Oxidation of amines by flavoproteins. Arch Biochem Biophys. 2010; 493:13–25. [PubMed: 19651103]
4. Mattevi A, Vanoni MA, Todone F, Rizzi M, Teplyakov A, Coda A, Bolognesi M, Curti B. Crystal structure of D-amino acid oxidase: A case of active site mirror-image convergent evolution with flavocytochrome b_2. Proc Natl Acad Sci USA. 1996; 93:7496–7501. [PubMed: 8755502]
5. Settembre EC, Dorrestein PC, Park J, Augustine AM, Begley TP, Ealick SE. Structural and mechanistic studies on *thiO*, a glycine oxidase essential for thiamin biosynthesis in *Bacillus subtilis*. Biochemistry. 2003; 42:2971–2981. [PubMed: 12627963]
6. Trickey P, Wagner MA, Jorns MS, Mathews FS. Monomeric sarcosine oxidase: structure of a covalently flavinylated amine oxidizing enzyme. Structure. 1999; 7:331–345. [PubMed: 10368302]
7. Leys D, Basran J, Scrutton NS. Channelling and formation of ‘active’ formaldehyde in dimethylglycine oxidase. EMBO J. 2003; 22:4038–4048. [PubMed: 12912903]
8. Khanna P, Schuman Jorns M. Characterization of the FAD-containing N-methyltryptophan oxidase from *Escherichia coli*. Biochemistry. 2001; 40:1441–1450. [PubMed: 11170472]
9. Binda C, Newton-Vinson P, Hubalek F, Edmondson DE, Mattevi A. Structure of human monoamine oxidase B, a drug target for the treatment of neurological disorders. Nat Struct Biol. 2002; 9:22–26. [PubMed: 11753429]
10. De Colibus L, Li M, Binda C, Lustig A, Edmondson DE, Mattevi A. Three-dimensional structure of human monoamine oxidase A (MAO A): relation to the structures of rat MAO A and human MAO B. Proc Natl Acad Sci U S A. 2005; 102:12684–12689. [PubMed: 16129825]
11. Stavropoulos P, Blobel G, Hoelz A. Crystal structure and mechanism of human lysine-specific demethylase-1. Nat Struct Mol Biol. 2006; 13:626–632. [PubMed: 16799558]
12. Faust A, Niefind K, Hummel W, Schomburg D. The structure of a bacterial L-amino acid oxidase from *Rhodococcus opacus* gives new evidence for the hydride mechanism for dehydrogenation. J Mol Biol. 2007; 367:234–248. [PubMed: 17234209]
13. Huang Q, Liu Q, Hao Q. Crystal structures of Fms1 and its complex with spermine reveal substrate specificity. J Mol Biol. 2005; 348:951–959. [PubMed: 15843025]
14. Seiler N. Catabolism of polyamines. Amino Acids. 2004; 26:217–233. [PubMed: 15221502]
15. White WH, Gunyuzlu PL, Toyn JH. *Saccharomyces cerevisiae* Is Capable of *de Novo* Pantothenic Acid Biosynthesis Involving a Novel Pathway of β-Alanine Production from Spermine. J Biol Chem. 2001; 276:10794–10800. [PubMed: 11154694]
16. Cervelli M, Polticelli F, Federico R, Mariottini P. Heterologous expression and characterization of mouse spermine oxidase. J Biol Chem. 2003; 278:5271–5276. [PubMed: 12458219]
17. Wu T, Yankovskaya V, McIntire WS. Cloning, sequencing, and heterologous expression of the murine peroxisomal flavoprotein, N1-acetylated polyamine oxidase. J Biol Chem. 2003; 278:20514–20525. [PubMed: 12660232]
18. Landry J, Sternglanz R. Yeast Fms1 is a FAD-utilizing polyamine oxidase. Biochem Biophys Res Commun. 2003; 303:771–776. [PubMed: 12670477]

19. Henderson Pozzi M, Gawandi V, Fitzpatrick PF. pH Dependence of a Mammalian Polyamine Oxidase: Insights into Substrate Specificity and the Role of Lysine 315. Biochemistry. 2009; 48:1508–1516. [PubMed: 19199575]
20. Adachi MS, Juarez PR, Fitzpatrick PF. Mechanistic Studies of Human Spermine Oxidase: Kinetic Mechanism and pH Effects. Biochemistry. 2010; 49:386–392. [PubMed: 20000632]
21. Adachi MS, Torres JM, Fitzpatrick PF. Mechanistic Studies of the Yeast Polyamine Oxidase Fms1: Kinetic Mechanism, Substrate Specificity, and pH Dependence. Biochemistry. 2010; 49:10440–10448. [PubMed: 21067138]
22. CRC Handbook of Chemistry and Physics. Vol. 61. CRC Press; Boca Rotan: 1980.
23. Cleland WW. Statistical analysis of enzyme kinetic data. Methods Enzymol. 1979; 63:103–138. [PubMed: 502857]
24. Kabsch W. XDS. Acta Cryst. 2010; D66:125–132.
25. Evans P. Scaling and assessment of data quality. Acta Cryst. 2006; D62:72–82.
26. McCoy AJ, Grosse-Kunstleve RW, Adams PD, Winn MD, Storoni LC, Read RJ. Phaser crystallographic software. J Appl Cryst. 2007; 40:658–674. [PubMed: 19461840]
27. Adams PD, Afonine PV, Bunkóczi G, Chen VB, Davis IW, Echols N, Headd JJ, Hung L-W, Kapral GJ, Grosse-Kunstleve RW, McCoy AJ, Moriarty NW, Oeffner R, Read RJ, Richardson DC, Richardson JS, Terwilliger TC, Zwart PH. PHENIX: a comprehensive Python-based system for macromolecular structure solution. Acta Cryst. 2010; D66:213–221.
28. Emsley P, Cowtan K. Coot: model-building tools for molecular graphics. Acta Cryst. 2004; D60:2126–2132.
29. Cleland, WW. Enzyme kinetics as a tool for determination of enzyme mechanisms. In: Bernasconi, CF., editor. Investigation of Rates and Mechanism. 4. Vol. 6. John Wiley & Sons; New York: 1986. p. 791-870.
30. Brouwer AC, Kirsch JF. Investigation of diffusion-limited rates of chymotrypsin reactions by viscosity variation. Biochemistry. 1982; 21:1302–1307. [PubMed: 7074086]
31. Roth JP, Klinman JP. Catalysis of electron transfer during the activation of O_2 by the flavoprotein glucose oxidase. Proc Natl Acad Sci USA. 2003; 100:62–67. [PubMed: 12506204]
32. Ghanem M, Gadda G. On the catalytic role of the conserved active site residue His_{466} of choline oxidase. Biochemistry. 2005; 44:893–904. [PubMed: 15654745]
33. Gadda G, Fan F, Hoang JV. On the contribution of the positively charged headgroup of choline to substrate binding and catalysis in the reaction catalyzed by choline oxidase. Arch Biochem Biophys. 2006; 451:182–187. [PubMed: 16713988]
34. Jorns MS, Chen Z-w, Mathews FS. Structural Characterization of Mutations at the Oxygen Activation Site in Monomeric Sarcosine Oxidase. Biochemistry. 2010
35. Zhao G, Bruckner RC, Jorns MS. Identification of the Oxygen Activation Site in Monomeric Sarcosine Oxidase: Role of Lys265 in Catalysis. Biochemistry. 2008; 47:9124–9135. [PubMed: 18693755]
36. Henderson Pozzi M, Fitzpatrick PF. A lysine conserved in the monoamine oxidase family is involved in oxidation of the reduced flavin in mouse polyamine oxidase. Arch Biochem Biophys. 2010; 498:83–88. [PubMed: 20417173]
37. Denu JM, Fitzpatrick PF. pH and kinetic isotope effects on the oxidative half-reaction of D-amino-acid oxidase. J Biol Chem. 1994; 269:15054–15059. [PubMed: 7910822]
38. Emanuele JJ Jr, Fitzpatrick PF. Mechanistic studies of the flavoprotein tryptophan 2-monooxygenase. 2. pH and kinetic isotope effects. Biochemistry. 1995; 34:3716–3723. [PubMed: 7893668]
39. Fitzpatrick PF. Substrate dehydrogenation by flavoproteins. Acc Chem Res. 2001; 34:299–307. [PubMed: 11308304]
40. Edmondson DE, Binda C, Mattevi A. Structural insights into the mechanism of amine oxidation by monoamine oxidases A and B. Arch Biochem Biophys. 2007; 464:269–276. [PubMed: 17573034]
41. Gaweska H, Henderson Pozzi M, Schmidt DMZ, McCafferty DG, Fitzpatrick PF. Use of pH and Kinetic Isotope Effects to Establish Chemistry As Rate-Limiting in Oxidation of a Peptide Substrate by LSD1. Biochemistry. 2009; 48:5440–5445. [PubMed: 19408960]

42. Fitzpatrick PF. Carbanion versus hydride transfer mechanisms in flavoprotein-catalyzed dehydrogenations. Bioorg Chem. 2004; 32:125–139. [PubMed: 15110192]

43. Ralph EC, Hirschi JS, Anderson MA, Cleland WW, Singleton DA, Fitzpatrick PF. Insights into the mechanism of flavoprotein-catalyzed amine oxidation from nitrogen isotope effects on the reaction of N-methyltryptophan oxidase. Biochemistry. 2007; 46:7655–7664. [PubMed: 17542620]

44. Ralph EC, Anderson MA, Cleland WW, Fitzpatrick PF. Mechanistic studies of the flavoenzyme tryptophan 2-monooxygenase: Deuterium and ^{15}N kinetic isotope effects on alanine oxidation by an L-amino acid oxidase. Biochemistry. 2006; 45:15844–15852. [PubMed: 17176107]

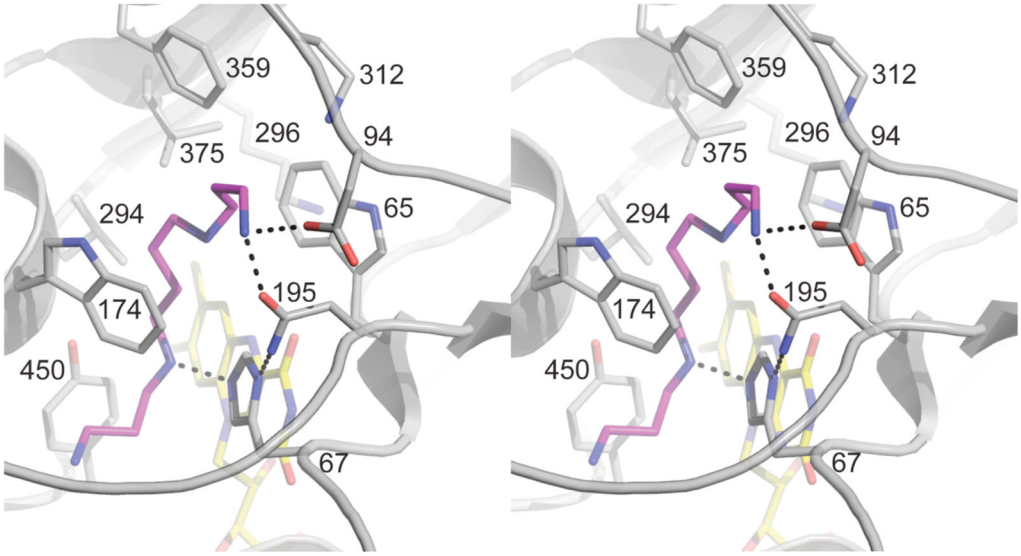

Figure 1.

Stereo view of the active site of *S. cerevisiae* Fms1 bond to spermine. The structure was drawn using subunit B of the pdb file 1xpq. The hydrogen bonds between amino acid side chains and spermine are those identified in reference (13).

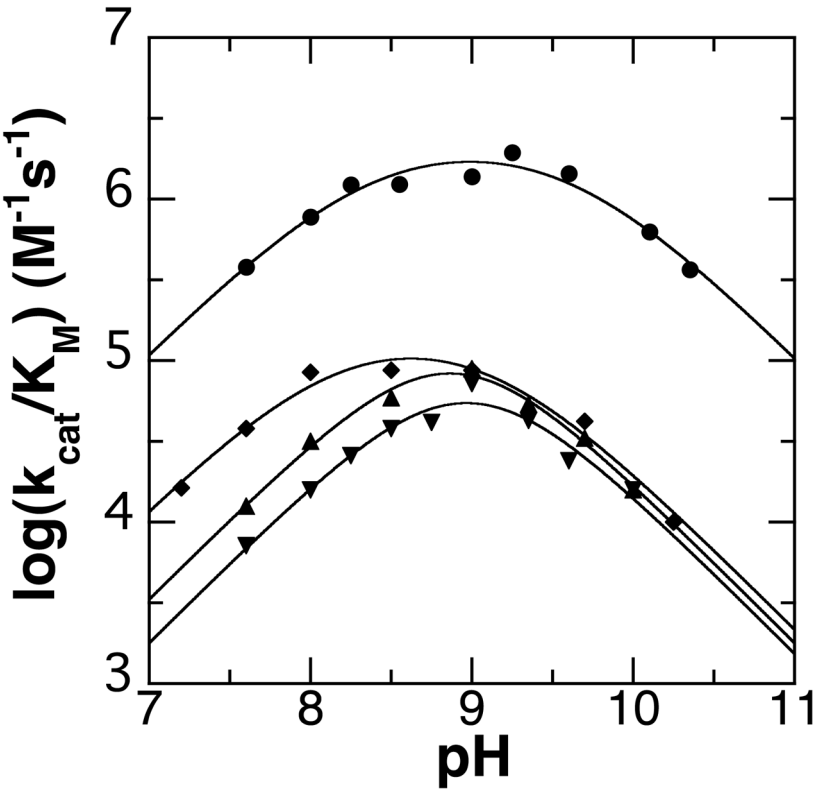

Figure 2.
Effect of pH on the k_{cat}/K_M value with N^1-acetylspermine as substrate for wild-type (●), H67Q (◆), H67A (▲), and H67N (▼) Fms1 at 25 °C. The lines are from fits of the data to eq 1. The data for the wild-type enzyme are from ref. 21.

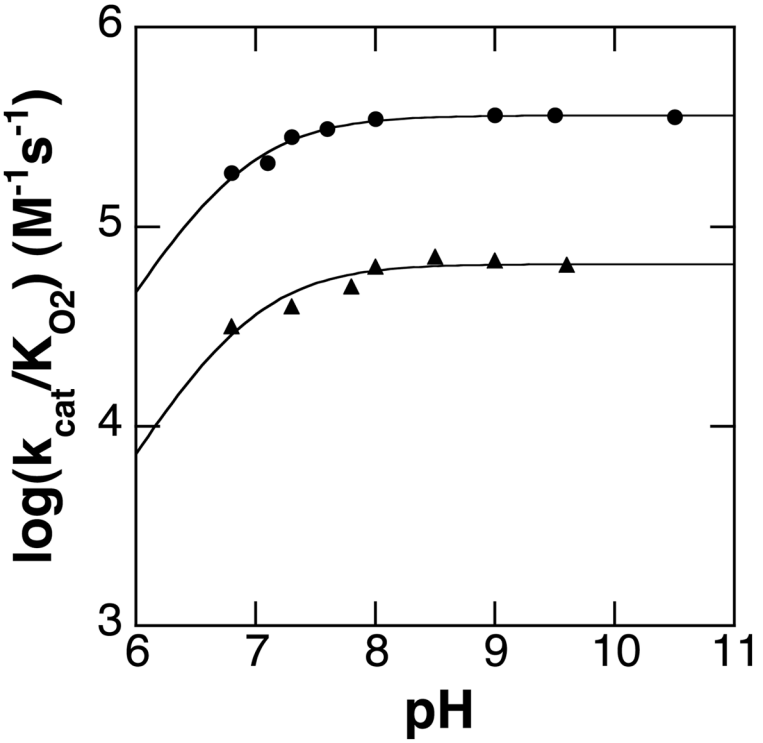

Figure 3.
Effect of pH on the k_{cat}/K_{O2} value for wild-type (●) and H67A (▲) Fms1 with N^1-acetylspermine as substrate at 25 °C. The lines are from fits to eq 2.

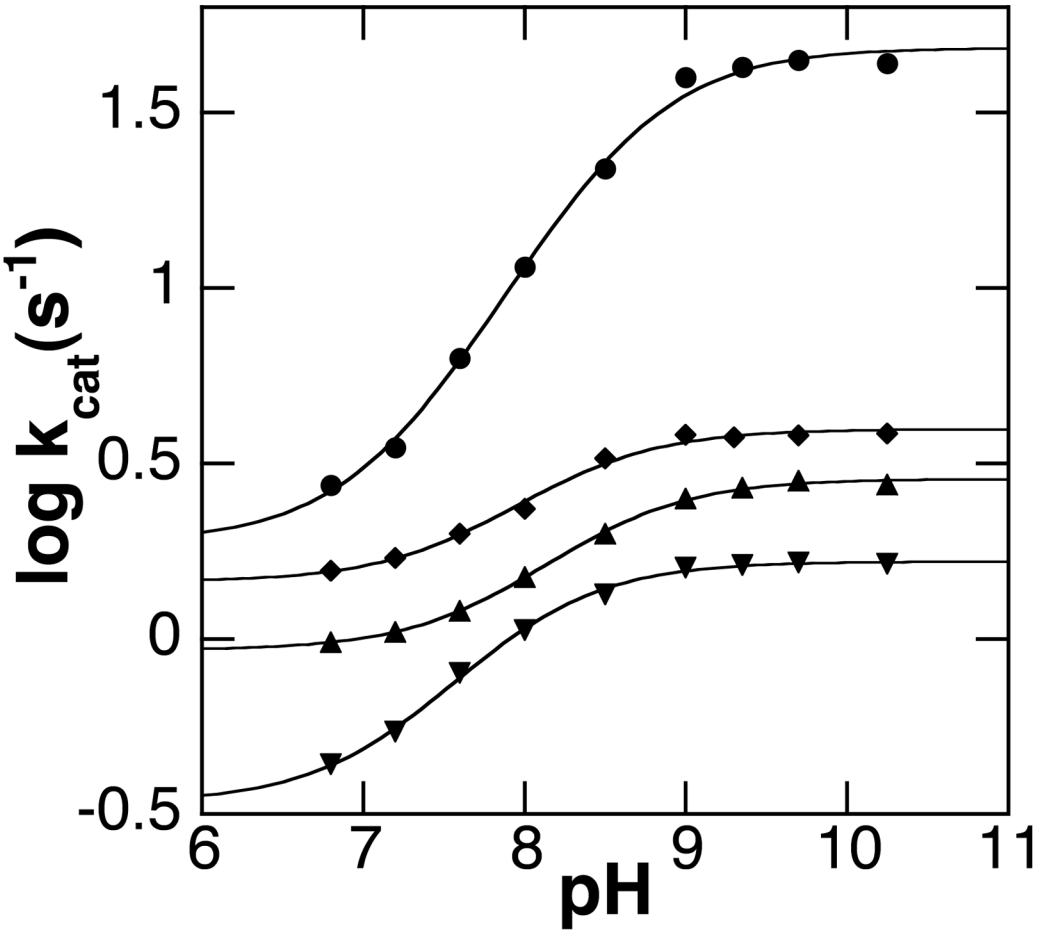

Figure 4.
Effect of pH on the k_{cat} value with N^1-acetylspermine for wild-type (●), H67Q (◆), H67A (▲), and H67N (▼) Fms1 at 25 °C. The lines are from fits to eq 3.

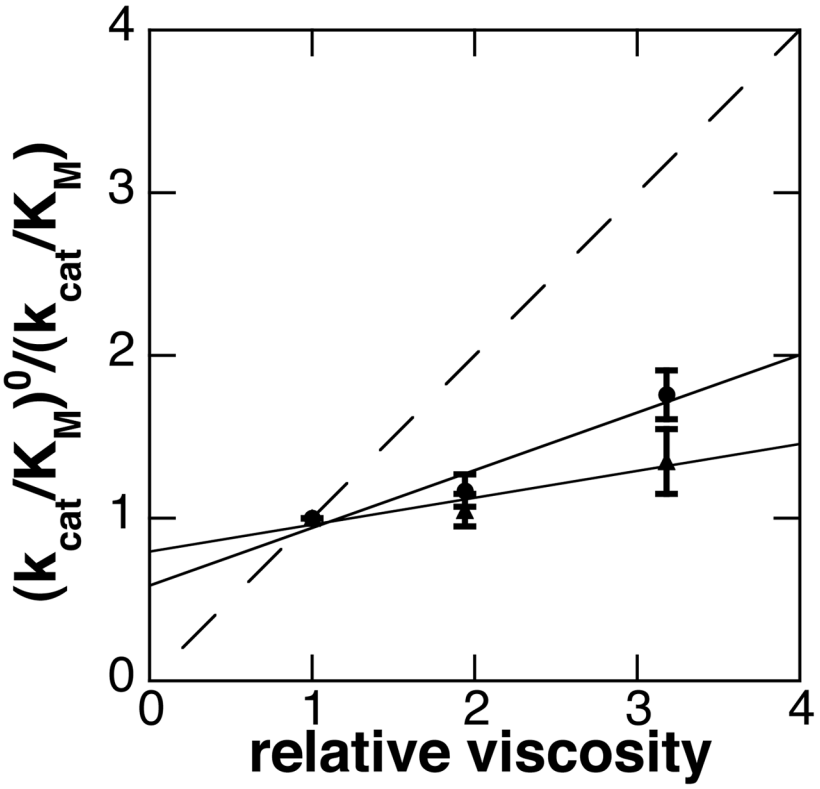

Figure 5.
Effect of solvent viscosity on the k_{cat}/K_M value with N^1-acetylspermine as a substrate for wild-type (●) and H67A (▲) Fms1 at pH 9.0, 25 °C. The solid lines are from linear regression fits. The dashed line shows the theoretical limit for a completely diffusion-limited reaction.

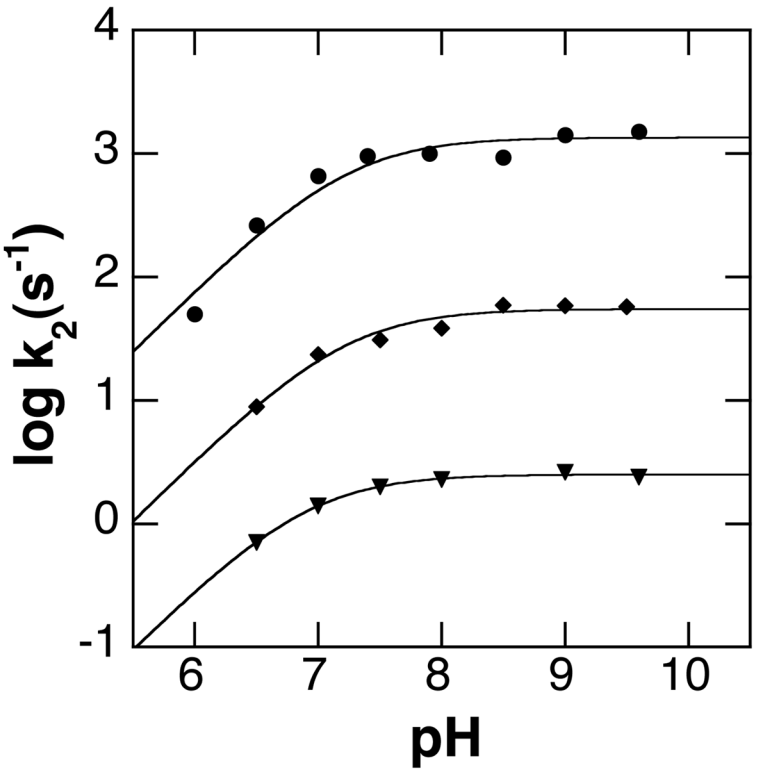

Figure 6.

Effect of pH on k_2, the limiting rate constant for reduction by N^1-acetylspermine, for wild-type (●), H67Q (◆), and H67N (▼) Fms1. The lines are from fits to eq 3. The data for the wild-type enzyme are from ref. 21 and were obtained at 4 °C. The data for the mutant enzymes were obtained at at 25 °C.

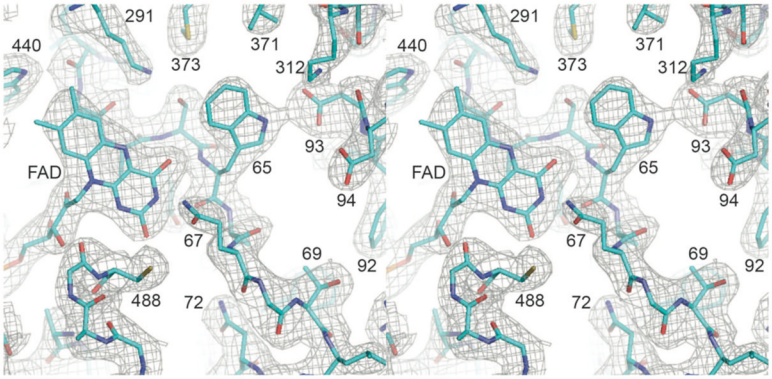

Figure 7.
The refined H67Q Fms1 structure superimposed onto a SIGMA-A weighted electron density map with coefficients 2*m*Fo-Fc and contoured at one sigma.

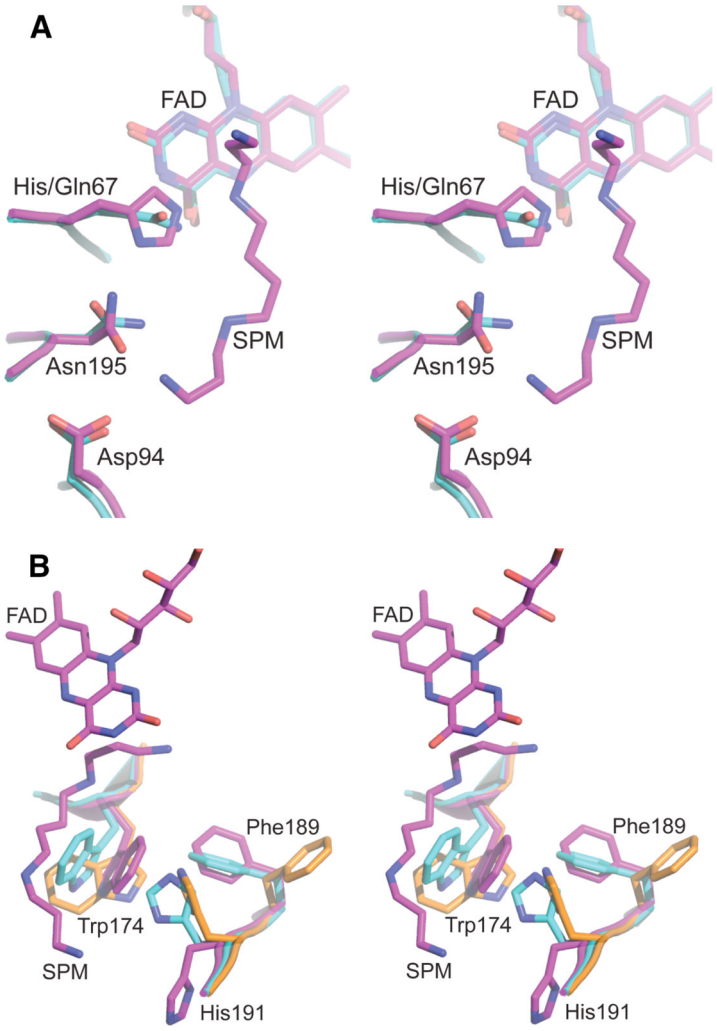

Figure 8.

Comparison of the active sites of wild-type and H67Q Fms1; orange carbons, wild-type Fms1; cyan carbons, H67Q Fms 1; magenta carbons, wild-type Fms1/spermine complex. For the free wild-type enzyme and the H6Q mutant protein, the structures are of the respective subunit A from pdb files 1yy5 and 4ech. For the spermine bound structure, Figure 8A is of subunit B and Figure 8B is of subunit C from pdb file 1xpq.

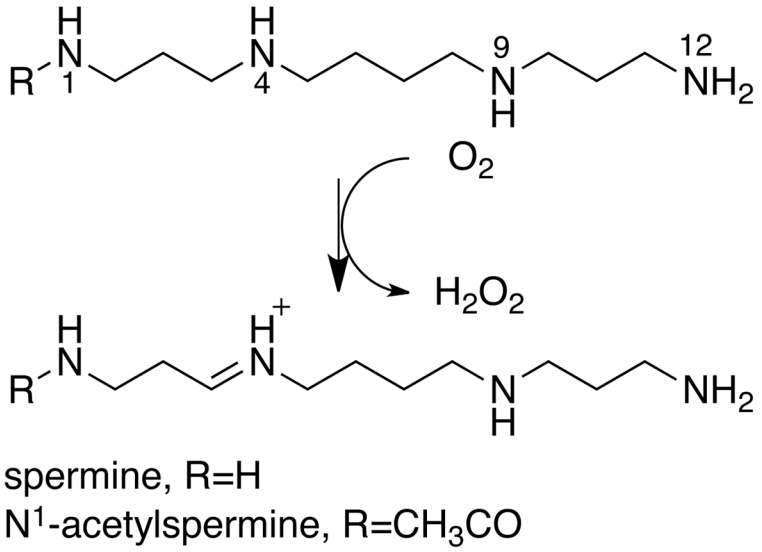

Scheme 1.

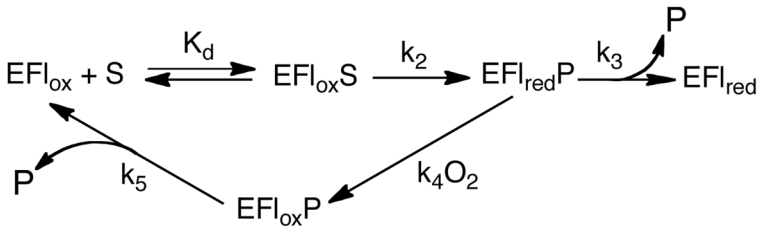

Scheme 2.

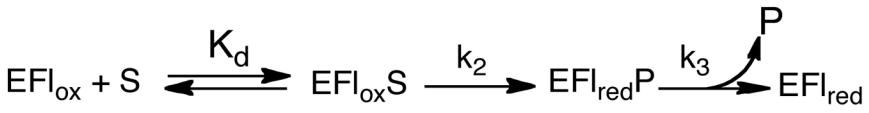

Scheme 3.

Table 1

Data collection and refinement statistics

Data collection	
space group	*C*2
cell dimensions	
a, *b*, *c* (Å)	161.2, 102.0, 75.8
α, β, γ (deg)	90, 93.1, 90
wavelength	0.9795
resolution (Å)	39.4 – 2.4
R_{sym} *	0.055 (0.531)
$I/\sigma I$	15.7 (2.7)
completeness (%)	99.6 (99.9)
redundancy	3.7 (3.8)
Refinement	
resolution (Å)	39.4 – 2.4 (2.53–2.40)
no. of reflections	47,724
R_{work}/R_{free}	0.214/0.266
Monomers per asymmetric unit	2
no. of atoms	
protein	7790
ligands	106
solvent	62
B-factors (Å^2)	
protein	65.7
ligands	47.5
solvent	51.1
rms deviations	
bond lengths (Å)	0.007
bond angles (deg)	1.112

*Values in parentheses are for the highest-resolution shell.

Table 2

Steady-State Kinetic Parameters for Wild-type and Mutant Fms1[a]

Substrate	Kinetic parameter	Fms1[d]	H67Q	H67N	H67A
N^1-acetylspermine[b]	k_{cat} (s^{-1})[c]	15.1 ± 0.4	3.9 ± 0.1	1.35 ± 0.04	2.7 ± 0.1
	k_{cat}/K_{amine} (mM^{-1} s^{-1})[c]	1400 ± 200	83 ± 11	72.5 ± 15.0	54 ± 14
	K_{amine} (μM)[c]	10.9 ± 1.8	47 ± 6	18.6 ± 4.0	50 ± 13
	k_{cat}/K_{O2} (mM^{-1} s^{-1})[e]	358 ± 20	225 ± 30	61 ± 9	68 ± 6
	K_{O2} (μM)[e]	43.6 ± 2.3	17.3 ± 2.3	22 ± 3	40 ± 3
spermine[f]	k_{cat} (s^{-1})[c]	39.0 ± 1.5	0.88 ± 0.01	0.04 ± 0.01[g]	0.44 ± 0.03
	k_{cat}/K_{amine} (mM^{-1} s^{-1})[c]	330 ± 60	3.6 ± 0.6	ND[h]	0.25 ± 0.05
	K_{amine} (μM)[c]	118 ± 25	165 ± 25	ND	1740 ± 310
	k_{cat}/K_{O2} (mM^{-1} s^{-1})[i]	428 ± 77	27.5 ± 3.0	ND	12 ± 1
	K_{O2} (μM)[i]	91 ± 16	32 ± 2	ND	37 ± 2

[a] Conditions: 25 °C.

[b] Determined at pH 9.0.

[c] Determined by varying the concentration of the amine at 1.3 mM oxygen.

[d] From ref. (21).

[e] Determined by varying the concentration of oxygen at 20 mM N^1-acetylspermine.

[f] Determined at pH 9.35.

[g] Determined at 30 mM spermine.

[h] Not determined.

[i] Determined by varying the concentration of oxygen at 20 mM spermine.

Table 3

pK_a Values for Wild-type and Mutant Fms1[a]

Enzyme	eq	Kinetic parameter	pK_1	pK_2
wild-type Fms1[b]	1	k_{cat}/K_M	8.3 ± 0.1	9.6 ± 0.1
	3	k_{cat}	8.5 ± 0.04[c]	—
	2	k_{cat}/K_{O2}	6.8 ± 0.05	—
	2	k_2	7.2 ± 0.1[d]	—
H67Q	1	k_{cat}/K_M	8.1 ± 0.1	9.1 ± 0.1
	3	k_{cat}	8.2 ± 0.1	—
	2	k_2	7.2 ± 0.1	—
H67N	1	k_{cat}/K_M	8.9 ± 0.1	8.9 ± 0.1
	3	k_{cat}	7.9 ± 0.03	—
	2	k_2	6.9 ± 0.02	—
H67A	1	k_{cat}/K_M	8.9 ± 0.1	8.9 ± 0.1
	3	k_{cat}	8.4 ± 0.03	—
	2	k_{cat}/K_{O2}	6.9 ± 0.1	—

[a] Conditions: N^1-acetylspermine as a substrate, 25 °C.

[b] From ref. (21).

[c] In ref. (21) eq. 2 was used.

[d] Determined at 4 °C.

Table 4

Intrinsic Kinetic Parameters for Wild-Type and Mutant Fms1[a]

Substrate	Kinetic parameter	Fms1	H67Q	H67N	H67A
N^1-acetylspermine	k_2 (s^{-1})	5490 ± 90[b]	58 ± 3	2.6 ± 0.1	13.6 ± 0.6
	K_d (μM)	484 ± 83[c]	23 ± 1	22 ± 7	16 ± 5
	k_3 (s^{-1})	1.5 ± 0.1[b]	1.4 ± 0.1	-	1.5 ± 0.03
	k_4 ($mM^{-1}s^{-1}$)[d]	204 ± 7[c]	225 ± 30	61 ± 9	68 ± 6
	k_5 (s^{-1})	15.1 ± 0.5[c]	4.2 ± 0.3	ND[e]	3.4 ± 0.3
spermine	k_2 (s^{-1})	126 ± 3[c]	2.1 ± 0.5	ND	0.60 ± 0.03
	K_d (μM)	23 ± 8[c]	3300 ± 500	ND	275 ± 50
	k_3 (s^{-1})	4.5 ± 0.1[c]	0.1 ± 0.02	ND	0.05 ± 0.002
	k_4 ($mM^{-1}s^{-1}$)[d]	402 ± 15[c]	27.5 ± 3.0	ND	12 ± 1
	k_5 (s^{-1})	56.5 ± 3.4[c]	ND	ND	ND

[a] Determined at pH 9.0, 25 °C.

[b] Calculated by extrapolating to 25 °C the data collected over the temperature range 4–15°C.

[c] From ref. (21).

[d] The value corresponds to the k_{Cat}/K_{O2} value (Table 2).

[e] Not determined.